Simulating CME initiation and evolution: state-of-the-art

S. Poedts & B. van der Holst & C. Jacobs & E. Chané
& G. Dubey & D. Kimpe

Centre for Plasma Astrophysics
K.U.Leuven

2nd ESWW, ESTEC (NL), 15 November 2005

Space weather : solar drivers

- drivers are of **solar origin**: viz. transient phenomena superposed on the solar wind:
  - CMEs (most prominent)
  - eruptive flares
  - SEPs
  - ...
- basic physical mechanisms **not fully understood**
- predictions and forecasts **'can be improved'**

CMEs :

- typ. 400 km/s, $10^{12} - 10^{13}$ kg!
- $E = 10^{24} - 10^{25}$ Joule
- known since 30 yrs only!
- they play a crucial role in SW!

Solar wind modeling : recent developments

- CSEM (Univ. Michigan): **first coupled model** of the inner heliosphere extending from the low solar corona to the well beyond Earth orbit

⇒ Space Weather Modeling Framework (SWMF): a high-performance flexible computational tool that *enables coupling state-of-the art models of the solar corona, the solar wind and solar energetic particles*

(Gombosi et al. (2004), Tóth et al. (2005)

Other groups also developed advanced solar wind models, e.g.:

- Lionello et al. (2003): **3D MHD model of the solar corona and of the solar wind** (polytropic eq. improved by incorporating thermal conduction ($\parallel \mathbf{B}$), radiation losses, and heating into the energy eq.)

Recent developments

- Lee et al. (2004): extended the CISM heliospheric model CORHEL to 10 AU to investigate how well this **solar magnetogram-based** 3D MHD model describes the solar wind influence on Saturn's magnetosphere

- Odstrcil et al. (2004): coupled numerical wind model where
(1) the ambient solar wind is derived from coronal models utilizing photospheric magnetic field observations and
(2) transient disturbances are derived from geometrical and kinematic fitting of coronagraph observations of coronal mass ejections (CMEs)

Solar wind models @ CPA

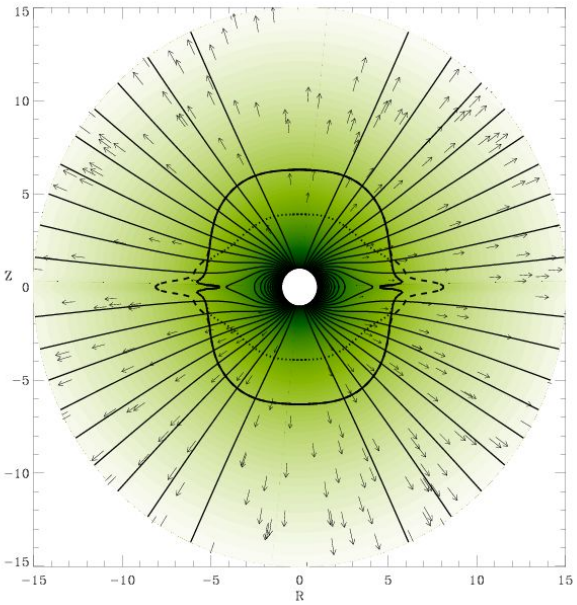

Polytropic Wind

Color: density (log-scale), black lines: magnetic field lines, arrows: velocity

Solar wind models @ CPA

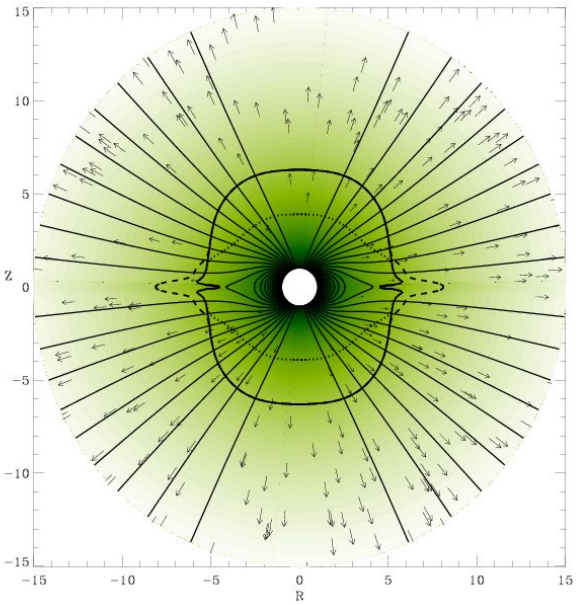

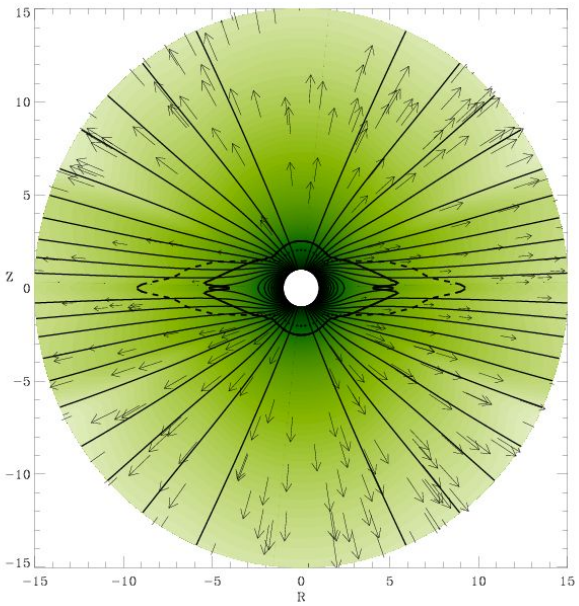

Polytropic Wind

Color: density (log-scale), black lines: magnetic field lines, arrows: velocity

'Manchester' wind

Extra heating source term:

$$Q = \rho q_0 e^{-\frac{(r-r_0)^2}{\sigma^2}} \left(T_0 - \gamma \frac{p}{\rho}\right)$$

Solar wind models @ CPA

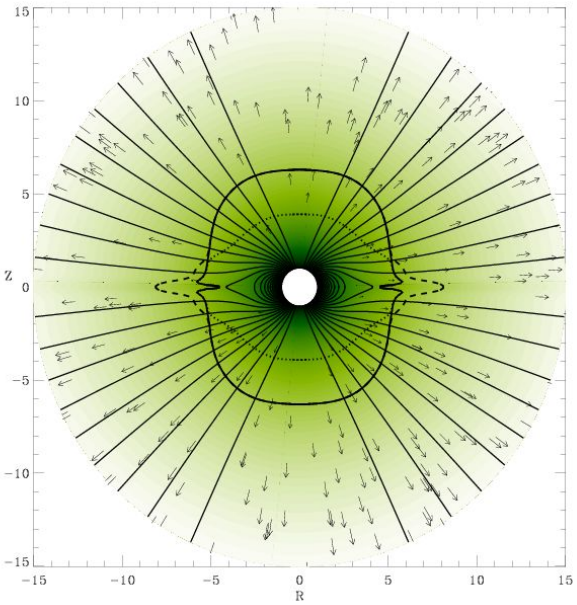

Polytropic Wind

Color: density (log-scale), black lines: magnetic field lines, arrows: velocity

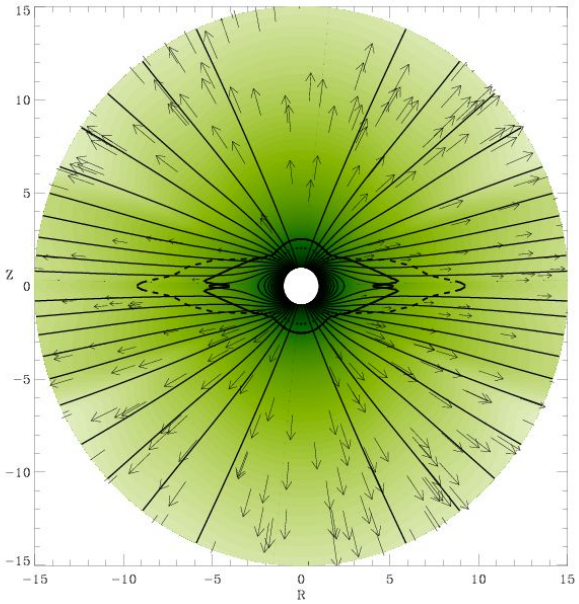

'Manchester' wind

Extra heating source term:

$$Q = \rho q_0 e^{-\frac{(r-r_0)^2}{\sigma^2}} \left(T_0 - \gamma \frac{p}{\rho}\right)$$

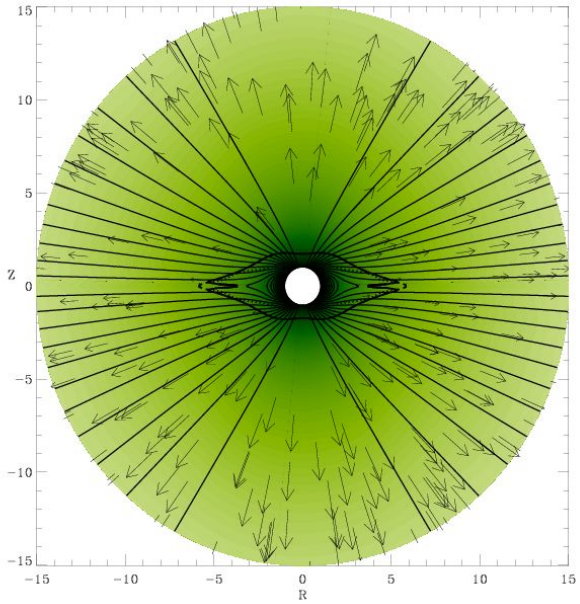

Polytropic Wind with Alfvén Waves

Has additional Alfvén wave pressure gradient.

Wind characteristics at $30R_\odot$

	Model 1	Model 2	Model 3
Density[m^{-3}]			
Pole	5.6×10^8	1.02×10^9	3.08×10^9
Equator	7.27×10^8	1.83×10^9	2.87×10^9
Ratio	0.77	0.56	1.07
Velocity[km/s]			
Pole	323	727	675
Equator	293	358	374
Ratio	**1.1**	**2.03**	**1.8**
Temperature[K]			
Pole	0.82×10^6	1.13×10^6	0.89×10^6
Equator	0.83×10^6	0.29×10^6	0.89×10^6
Ratio	0.99	3.87	1.0
Magnetic field[G]			
Pole	6.04×10^{-4}	3.7×10^{-4}	3.9×10^{-4}
Equator	6.1×10^{-5}	1.2×10^{-4}	2.0×10^{-4}
Ratio	9.89	3.06	1.95

Recent developments

- heliospheric models of CME propagation and evolution provide an **important insight into the dynamics of CMEs** and are a **valuable tool for interpreting interplanetary in situ observations**

- Linker et al. (2003): **need to study coronal initiation and solar wind propagation together**

  $\Rightarrow$ serious efforts have been undertaken to reach this goal!

- Roussev et al. (2003a,b) developed the capability to use observed **synoptic magnetograms** to drive the coupled corona-solar-wind model and to simulate the SW. The tool was used to simulate a 3D flux-rope model for a CME **based on a loss of equilibrium**, i.e. not on an initially unsatisfied force balance as in many earlier (and current) simulations!

Recent developments (cont.)

- Manchester et al. (2004a,b) also modeled erupting flux ropes and the resulting CMEs in **full 3D magnetohydrodynamics**
- Sokolov et al. (2004) then included a field line advection model and this coupled corona-solar-wind-SEP model thus **includes the energetic particle environment** at any point in the inner heliosphere in the simulations
- Manchester et al. (2005) focussed on the **CME shock and sheat structures** relevant for particle acceleration, while Lugaz et al. (2005) concentrated on the **evolution of the density structure of the CMEs**

Recent developments (cont.)

- Jacobs et al. (2005) also focussed on the propagation of fast-CME generated MHD shock waves and made a first attempt to **quantify the effect of the background solar wind model** on this evolution by superposing the same simple CME model on three different 2.5D (axisymmetric) wind models
- Chané et al. (2005) then studied the **effect of the CME initiation parameters on the CME evolution**, in particular the polarity of the initial magnetic flux rope $\Rightarrow$ *affects velocity, path, spread angle, etc.*

CME initiation: foot point shearing

Add extra azimuthal velocity v_ϕ^0 at the solar surface to shear the footpoints of the magnetic field.

magnetic field lines

$$v_\phi^0 = v_0(t)\Theta e^{(1-\Theta^4)/4}$$

$$\text{with } \Theta = \frac{\theta - \pi/2}{\Delta\theta_m}$$

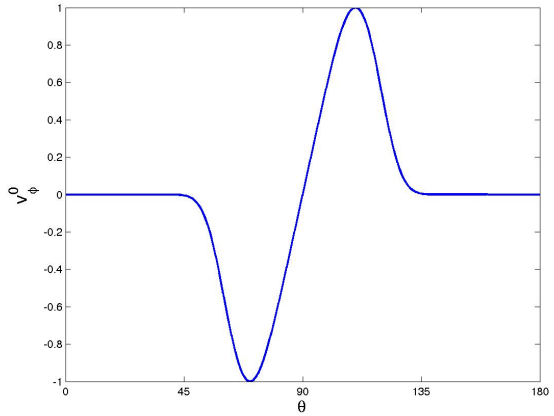

Background wind: Model 1, maximum shear velocity: 6 km/s.

CME initiation: Shearing

Add extra azimuthal velocity v_ϕ^0 at the solar surface to shear the footpoints of the magnetic field.

$$v_\phi^0 = v_0(t)\Theta e^{(1-\Theta^4)/4}$$

$$\text{with } \Theta = \frac{\theta - \pi/2}{\Delta\theta_m}$$

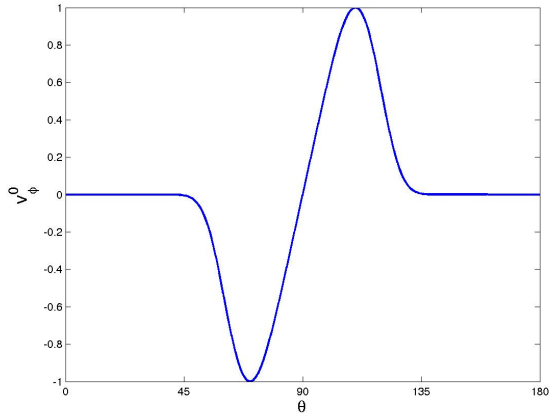

relative density $(\rho - \rho_{wind})/\rho_{wind}$

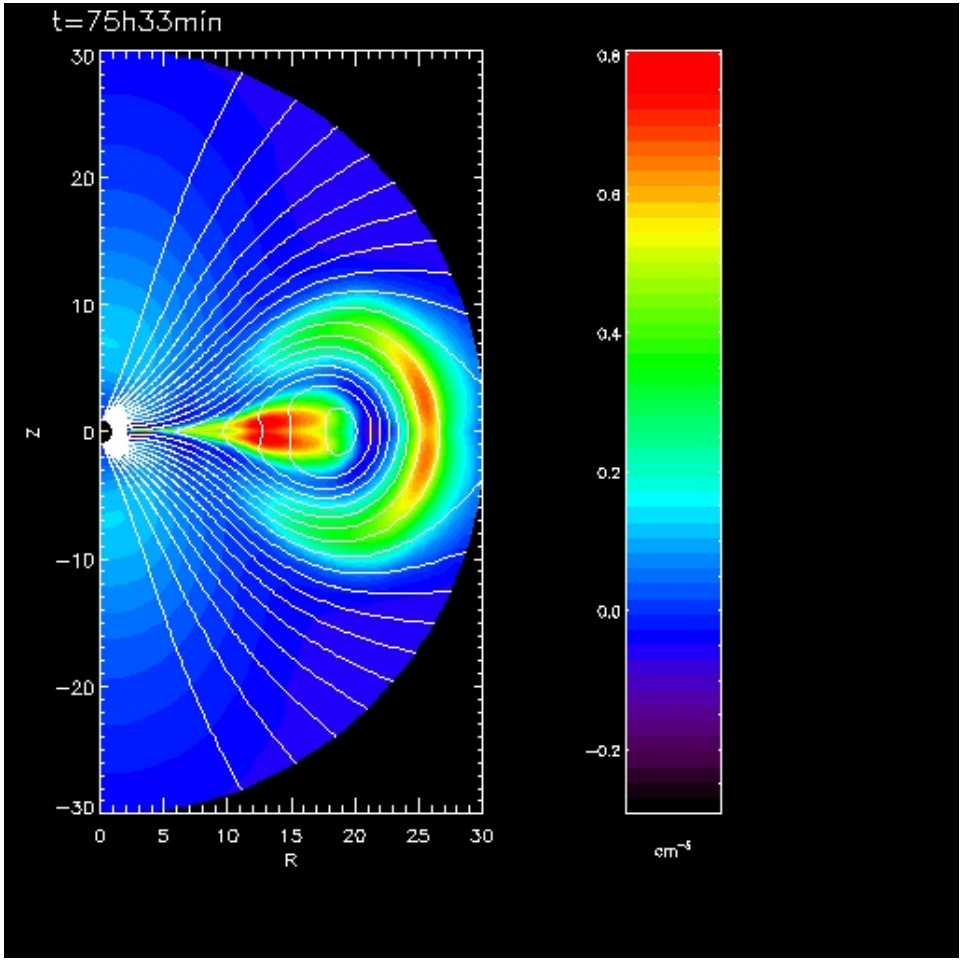

Background wind: Model 1, maximum shear velocity: 6 km/s.

CME initiation: Shearing - parameter studies

Shearing rate & background wind both affect

- Δt to reach instability
- instability threshold in terms of energy
- amount of energy released
- velocity/acceleration of flux rope
- ...

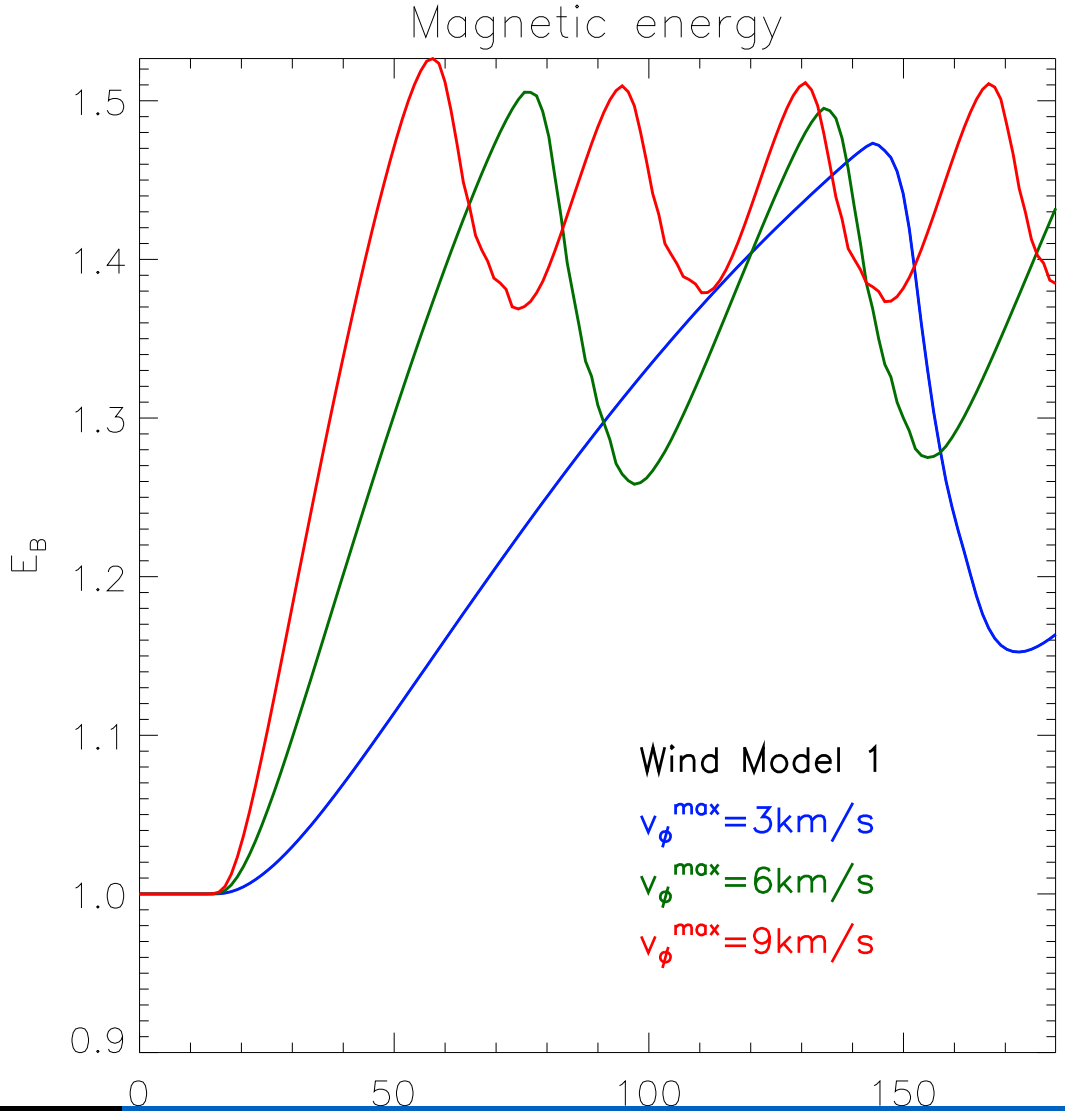

CME initiation: Shearing - parameter studies

Shearing rate & background wind both affect

- Δt to reach instability
- instability threshold in terms of energy
- amount of energy released
- velocity/acceleration of flux rope
- ...

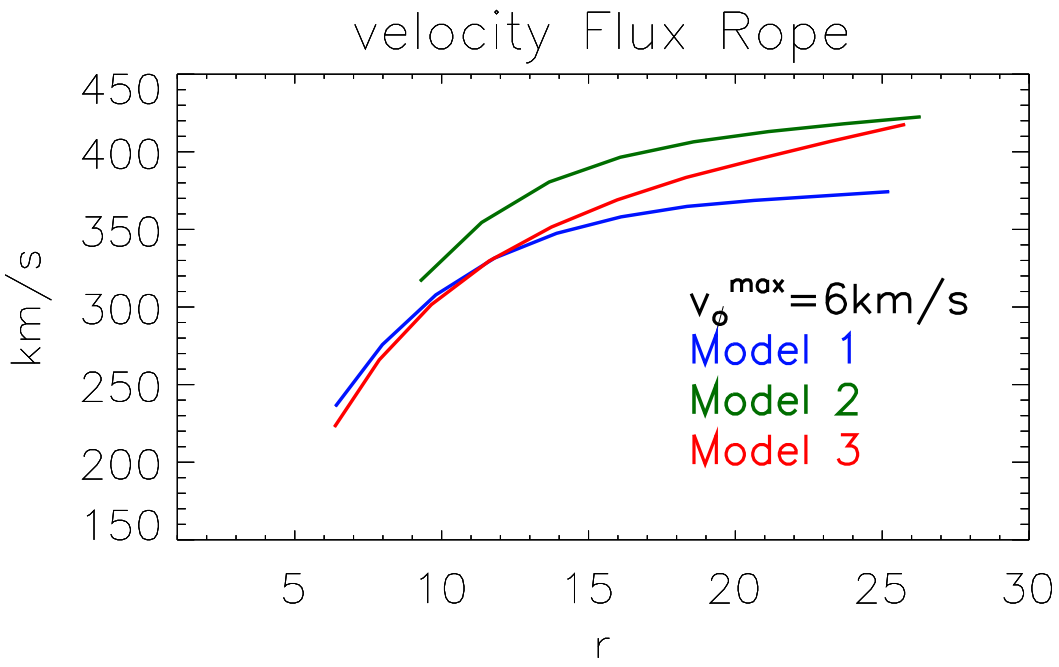

Magnetic helicity

$$H_r = \int_V (\mathbf{A}+\mathbf{A}_p)\cdot(\mathbf{B}-\mathbf{B}_p)dV$$

simplifies to

$$H_r = 2\int_V A_\varphi B_\varphi dV$$

in axi-symmetric case

⇒ **easy to compute**
⇒ **difficult to measure!**
⇒ *helicity injection rate*

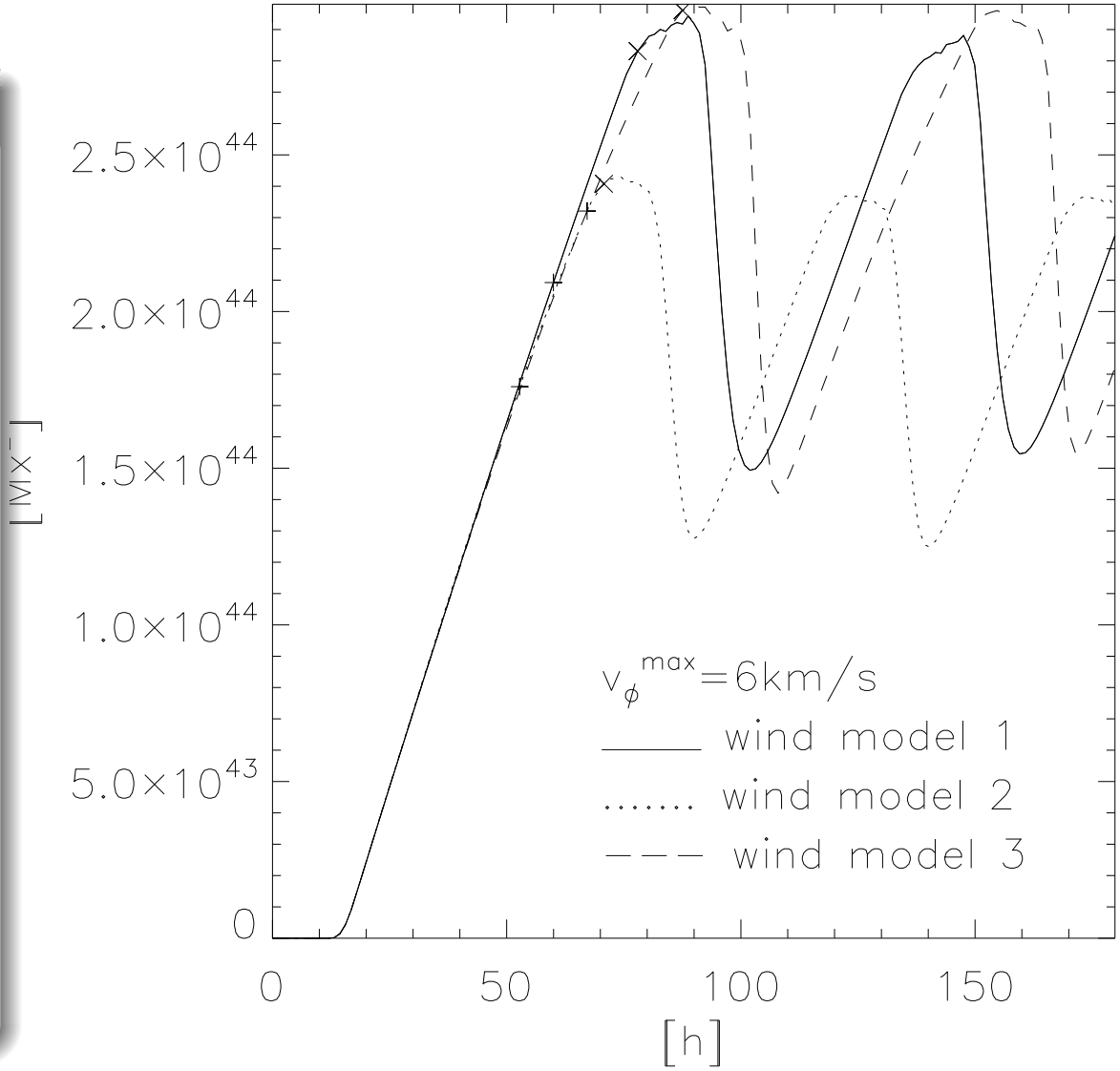

Magnetic helicity

$$H_r = \int_V (\mathbf{A}+\mathbf{A}_p)\cdot(\mathbf{B}-\mathbf{B}_p)dV$$

simplifies to

$$H_r = 2\int_V A_\varphi B_\varphi dV$$

in axi-symmetric case

⇒ **easy to compute**
⇒ **difficult to measure!**
⇒ *helicity injection rate*

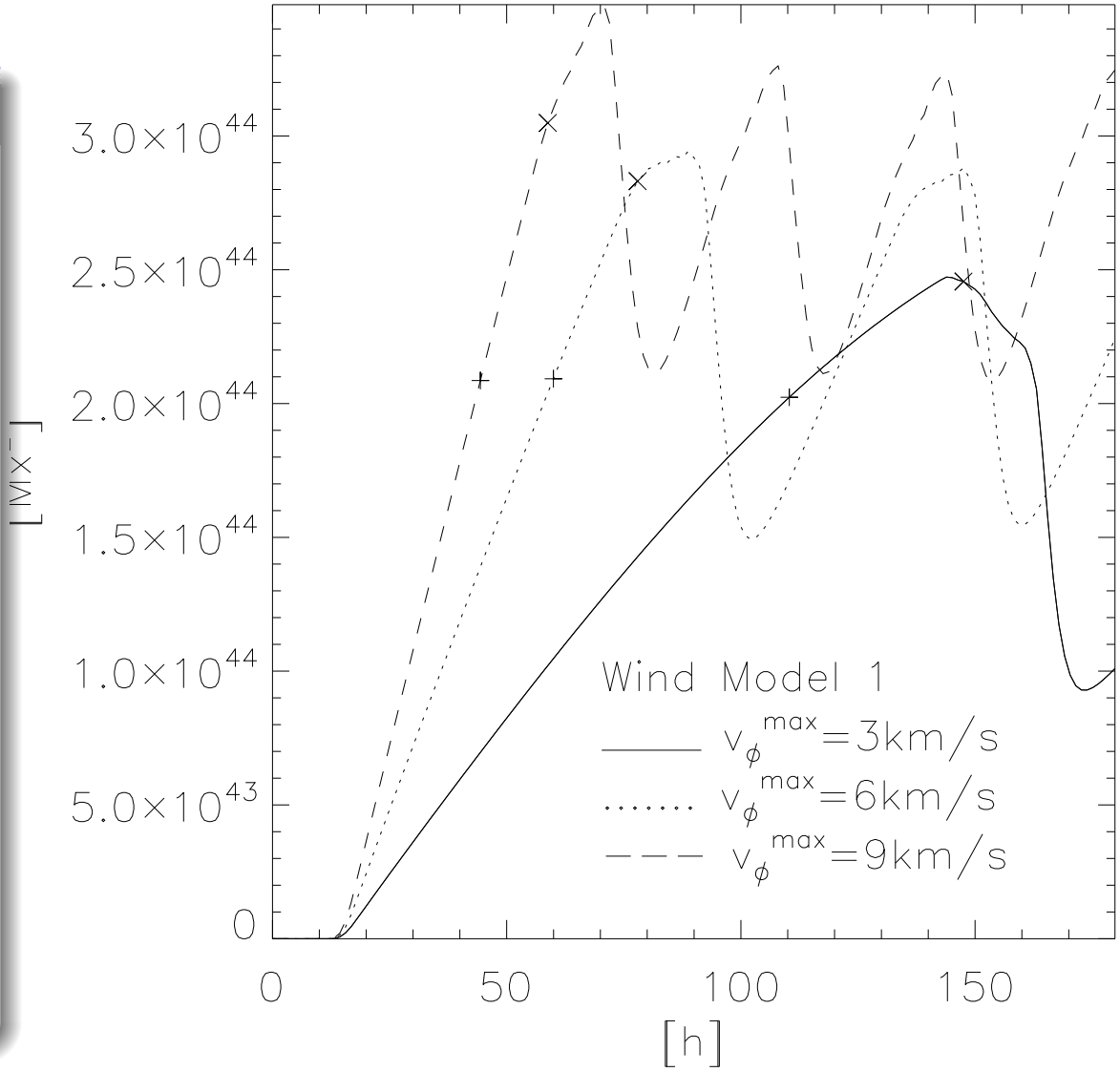

Magnetic helicity

$$H_r = \int_V (\mathbf{A}+\mathbf{A}_p)\cdot(\mathbf{B}-\mathbf{B}_p)dV$$

simplifies to

$$H_r = 2\int_V A_\varphi B_\varphi dV$$

in axi-symmetric case

⇒ **easy to compute**
⇒ **difficult to measure!**
⇒ *helicity injection rate*

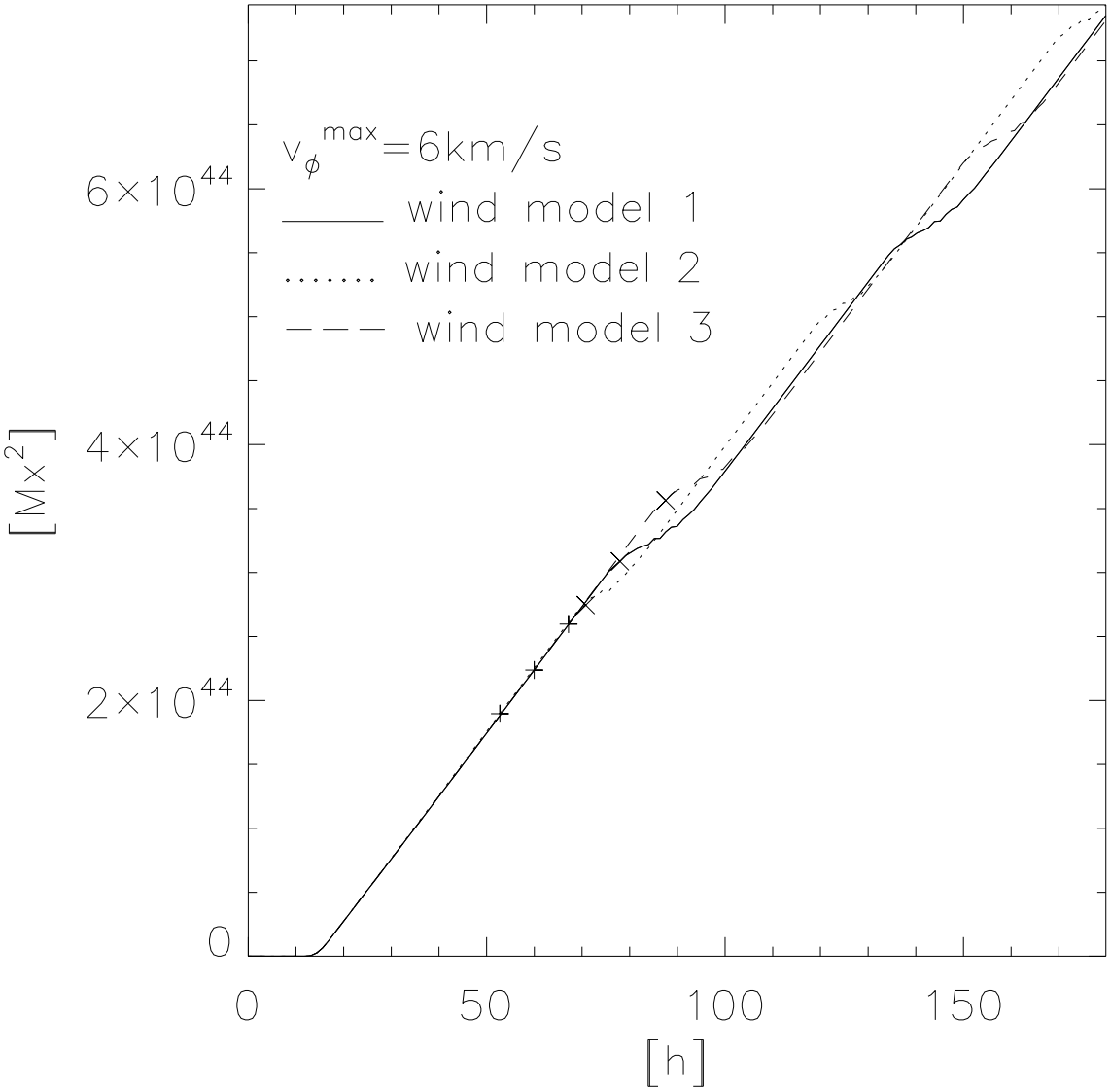

Magnetic helicity

$$H_r = \int_V (\mathbf{A}+\mathbf{A}_p)\cdot(\mathbf{B}-\mathbf{B}_p)dV$$

simplifies to

$$H_r = 2\int_V A_\varphi B_\varphi dV$$

in axi-symmetric case

⇒ **easy to compute**
⇒ **difficult to measure!**
⇒ *helicity injection rate*

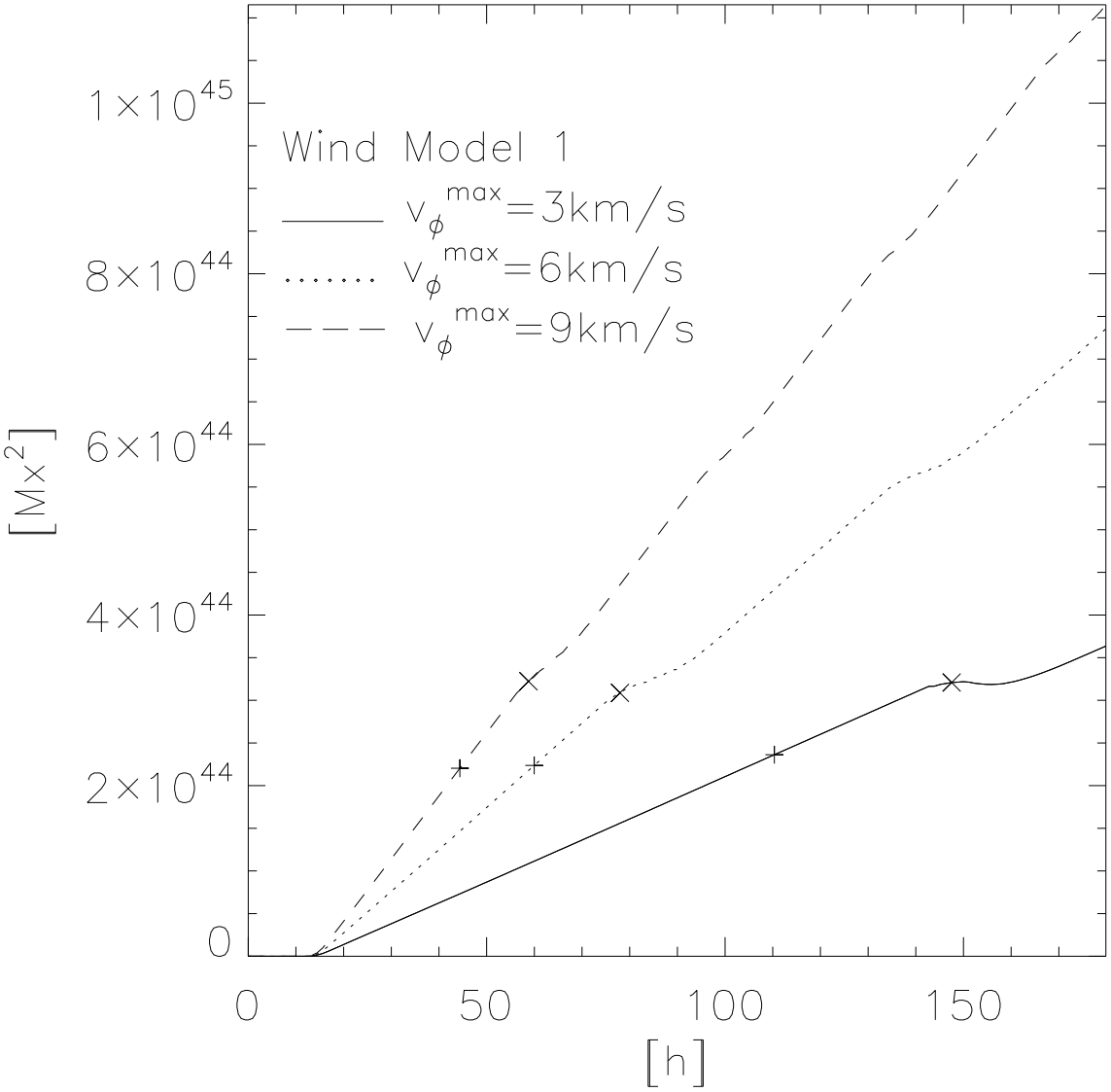

CME initiation: flux emergence / cancellation

Initial model

- cf. Chen & Shibata (2000)
- + **physics** : MHD (incl. gravity)
- + **geometry** : 2D (axisymmetric)
- + dipole field
  OR
  + **solar wind** $\Rightarrow$

$$\vec{B}_0 = \vec{B}_{\mathrm{LC}} + \vec{B}_{\mathrm{IC}} + \vec{B}_{\mathrm{BG}}$$

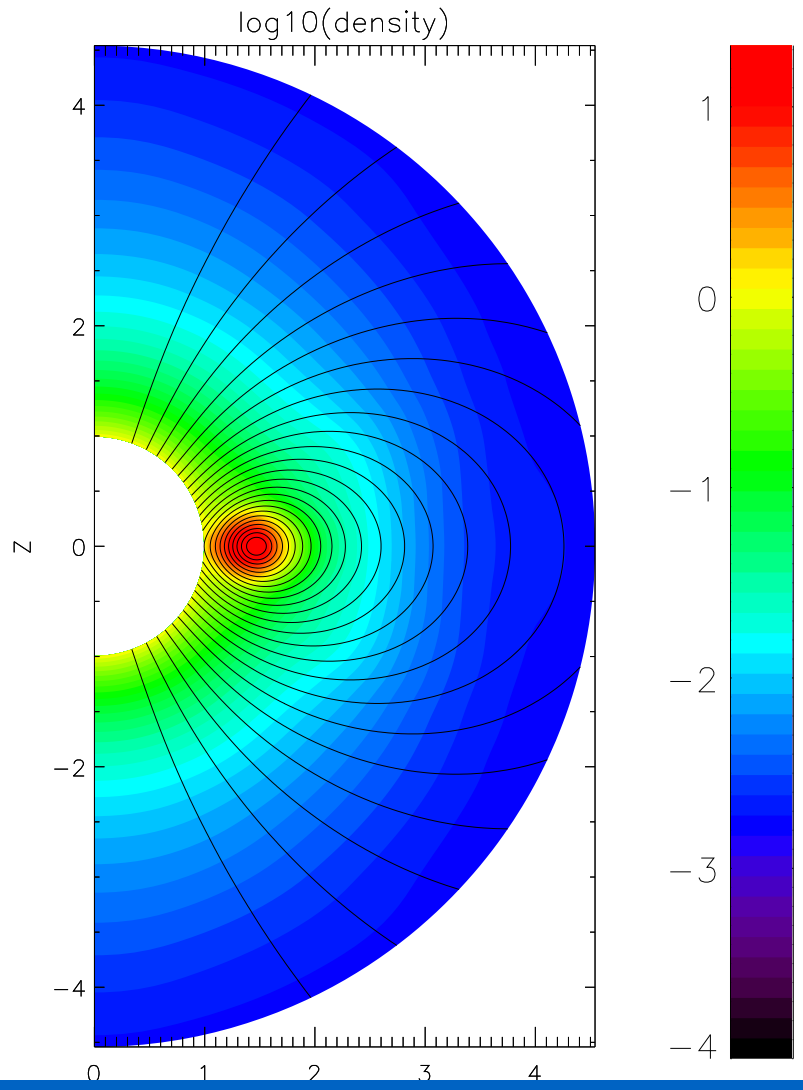

CME initiation: flux emergence / cancellation

Addition of flux

cf. Forbes & Priest ('84), Chen & Shibata ('00)

- at lower boundary ($r = 1R_\odot$)
- in region $\frac{\pi}{2} - 0.6 \leq \theta \leq \frac{\pi}{2} + 0.6$
- BC: $A_\varphi = A_\varphi(t_0) + c_e\, A_\varphi^+ \dfrac{t - t_0}{t_e - t_0}$

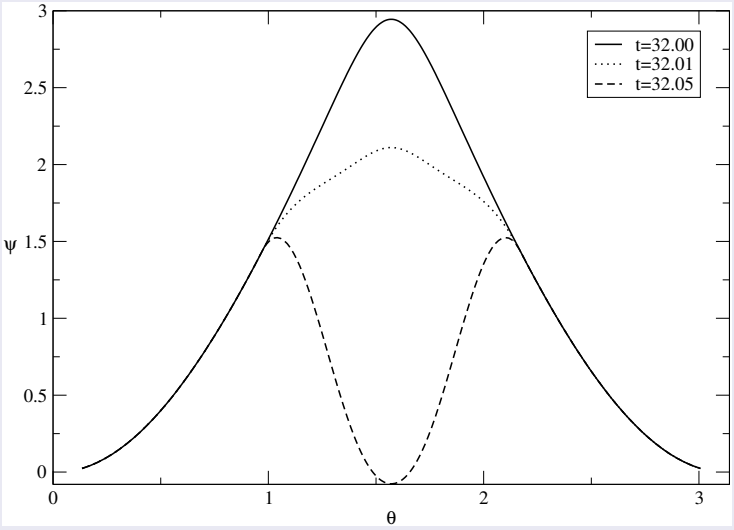

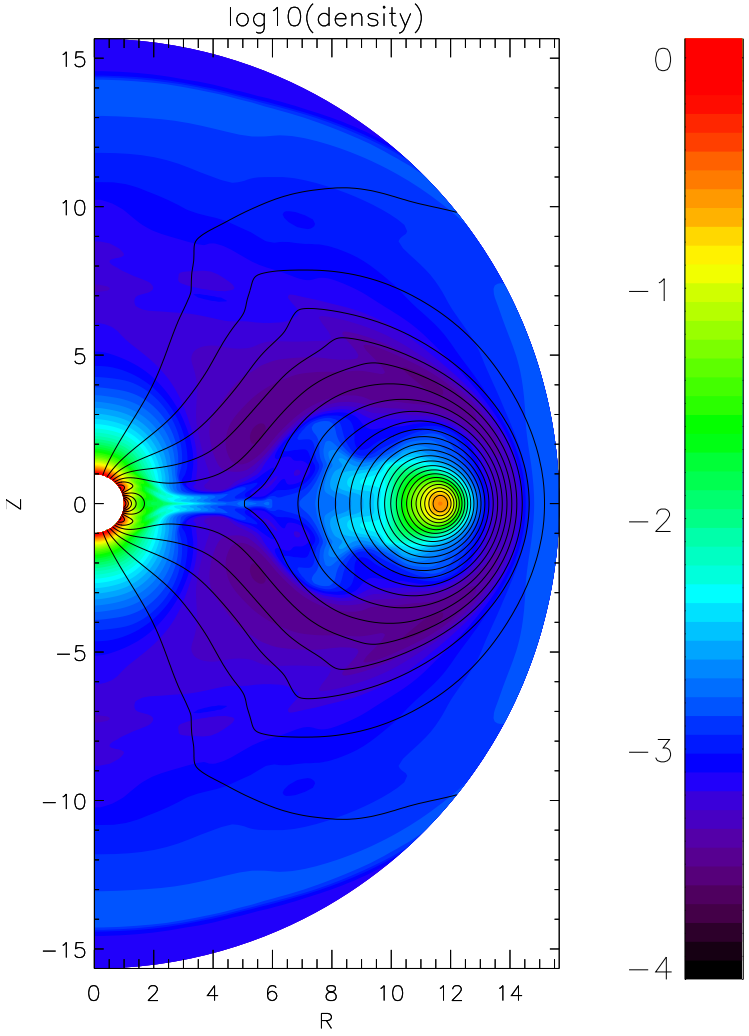

Case A : varying flux emergence rate, fixed c_e (total flux)

Parameter study : t_e

- BC:
  $$A_\varphi = A_\varphi(t_0) + c_e\, A_\varphi^+ \frac{t - t_0}{t_e - t_0}$$
- fixed amount of flux: $2\pi\, c_e\, \psi_0 \approx -6.6 \times 10^{22}$ Mx in Northern hemisphere
- vary *flux emergence rate*, i.e. $2\pi\, c_e\, \psi_0 / \Delta t$ from -1.10×10^{20} to -1.22×10^{19} Mx/s

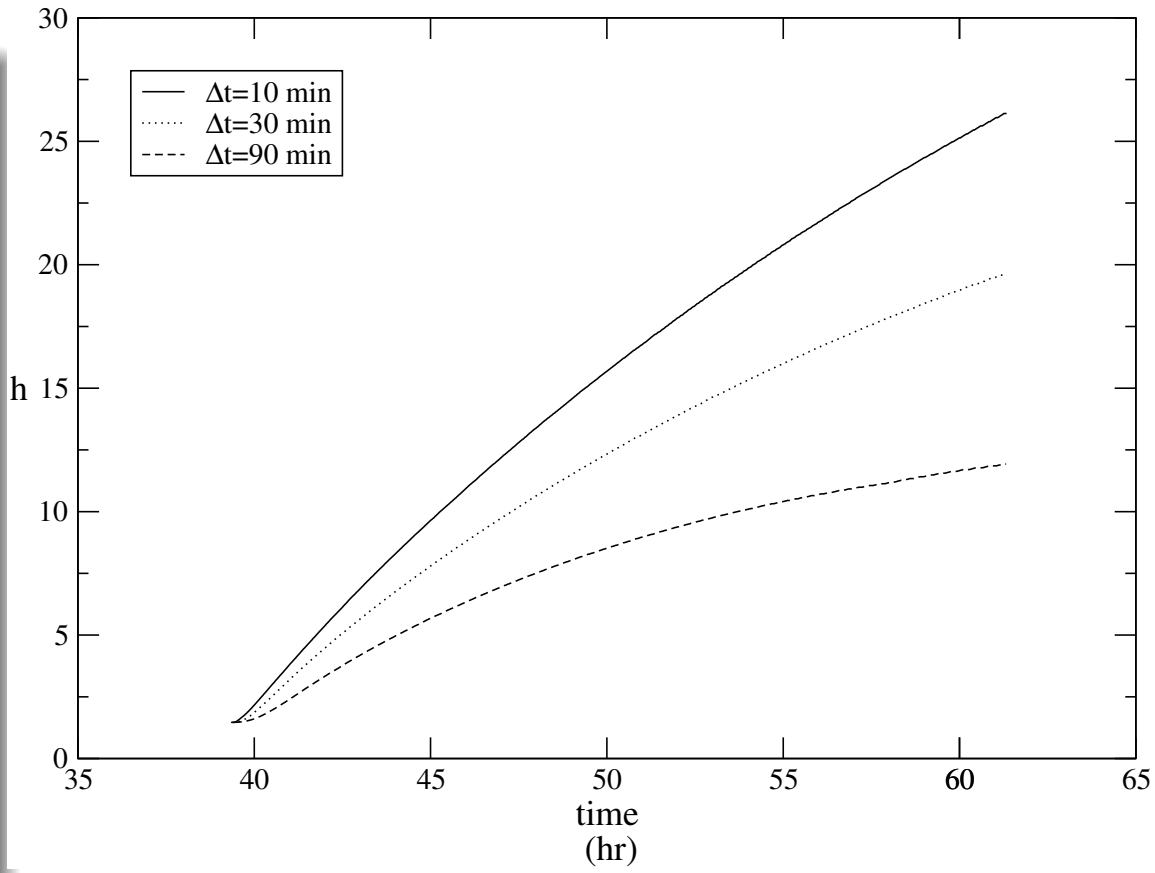

Height - time plot for difference flux emergence rates

Case A : varying flux emergence rate, fixed c_e (total flux)

Parameter study : t_e

- BC:
  $$A_\varphi = A_\varphi(t_0) + c_e\, A_\varphi^+ \frac{t - t_0}{t_e - t_0}$$
- fixed amount of flux: $2\pi\, c_e\, \psi_0 \approx -6.6 \times 10^{22}$ Mx in Northern hemisphere
- vary *flux emergence rate*, i.e. $2\pi\, c_e\, \psi_0 / \Delta t$ from -1.10×10^{20} to -1.22×10^{19} Mx/s

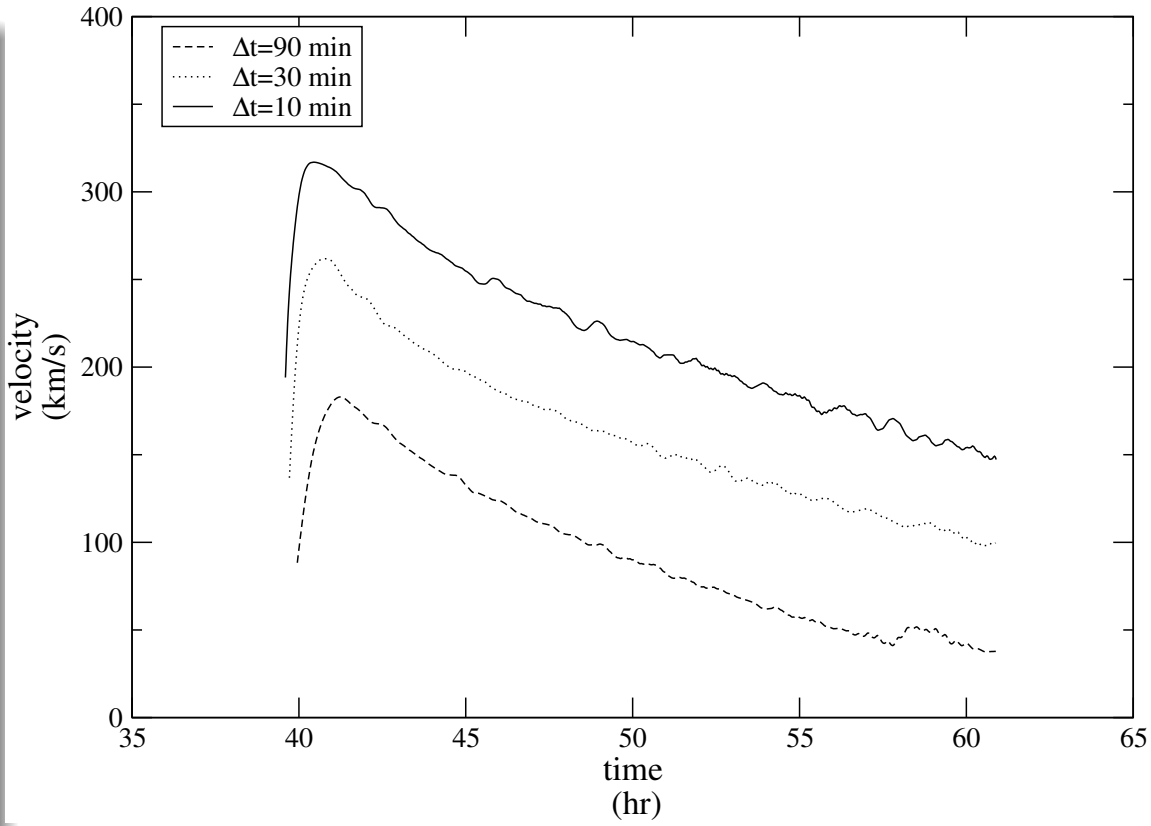

Velocity of the flux rope center vs. time

Case B : varying flux emergence rate, fixed t_e (Δt)

Parameter study : t_e

- fixed $\Delta t = 30$ min
- *total flux* varies from -1.1×10^{22} Mx ($c_e = -1$) to -9.9×10^{22} Mx ($c_e = -9$)
- *flux emergence rate* varies from -1.22×10^{19} to -1.10×10^{20} Mx/s

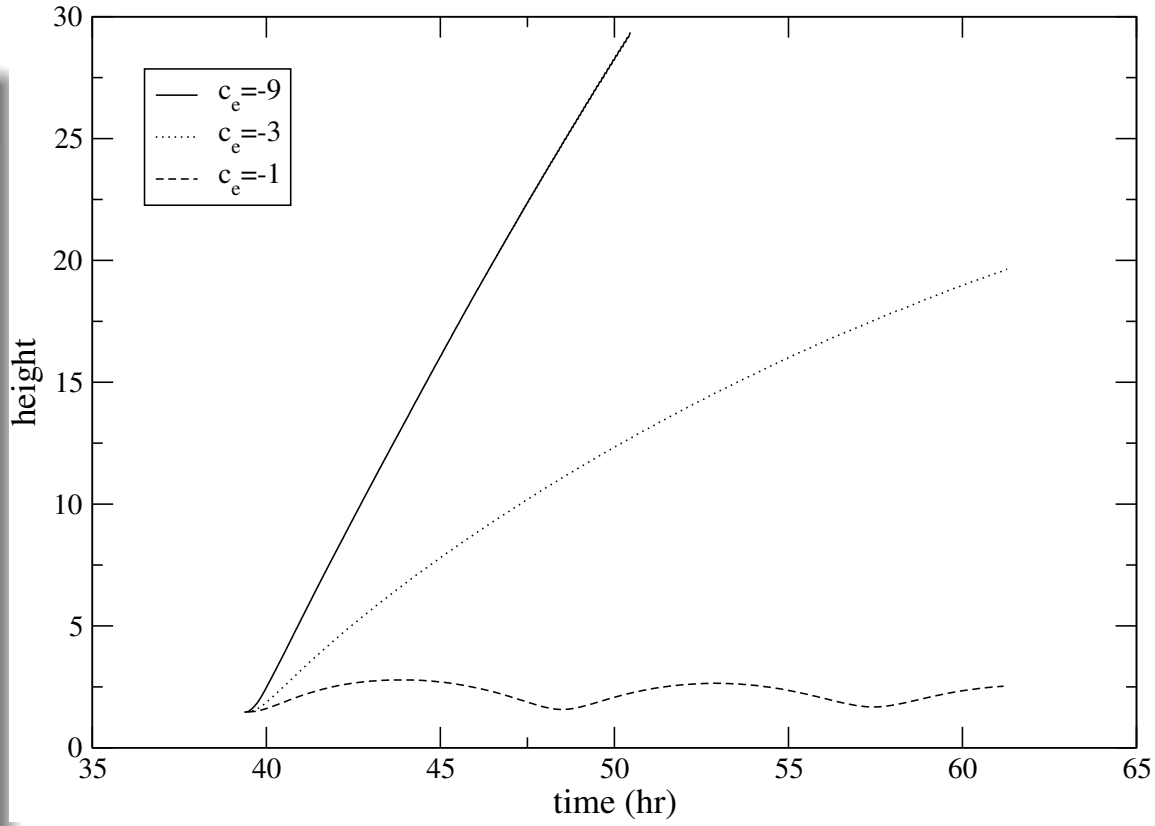

Height - time plot for difference flux emergence rates

Case B : varying flux emergence rate, fixed t_e (Δt)

Parameter study : t_e

- fixed $\Delta t = 30$ min
- *total flux* varies from -1.1×10^{22} Mx ($c_e = -1$) to -9.9×10^{22} Mx ($c_e = -9$)
- *flux emergence rate* varies from -1.22×10^{19} to -1.10×10^{20} Mx/s

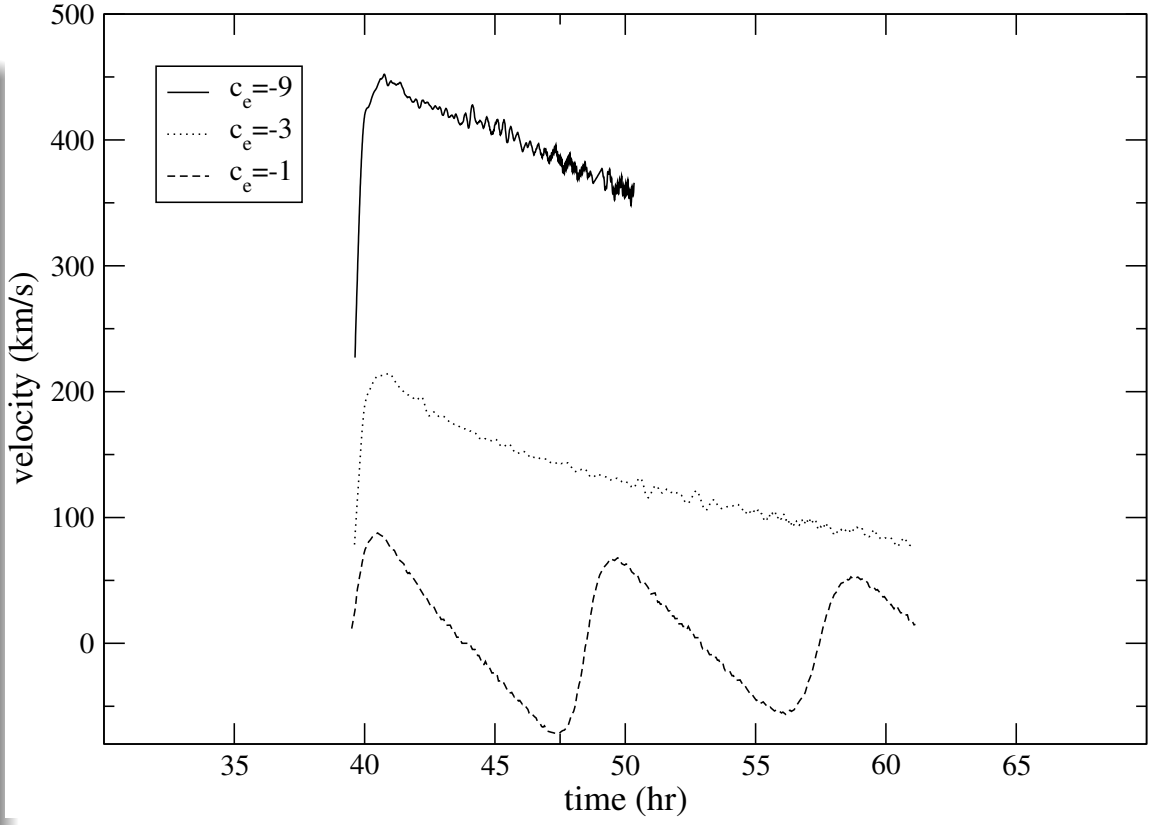

Velocity of the flux rope center vs. time

Case C : fixed flux emergence rate, varying t_e and c_e

	$\Delta t =$	10 min	30 min	90 min
	-1	3.67×10^{19} Mx/s	1.10×10^{20} Mx/s	
$c_e =$	-3	1.22×10^{19} Mx/s	3.67×10^{19} Mx/s	1.10×10^{20} Mx/s
	-9		1.22×10^{19} Mx/s	3.67×10^{19} Mx/s

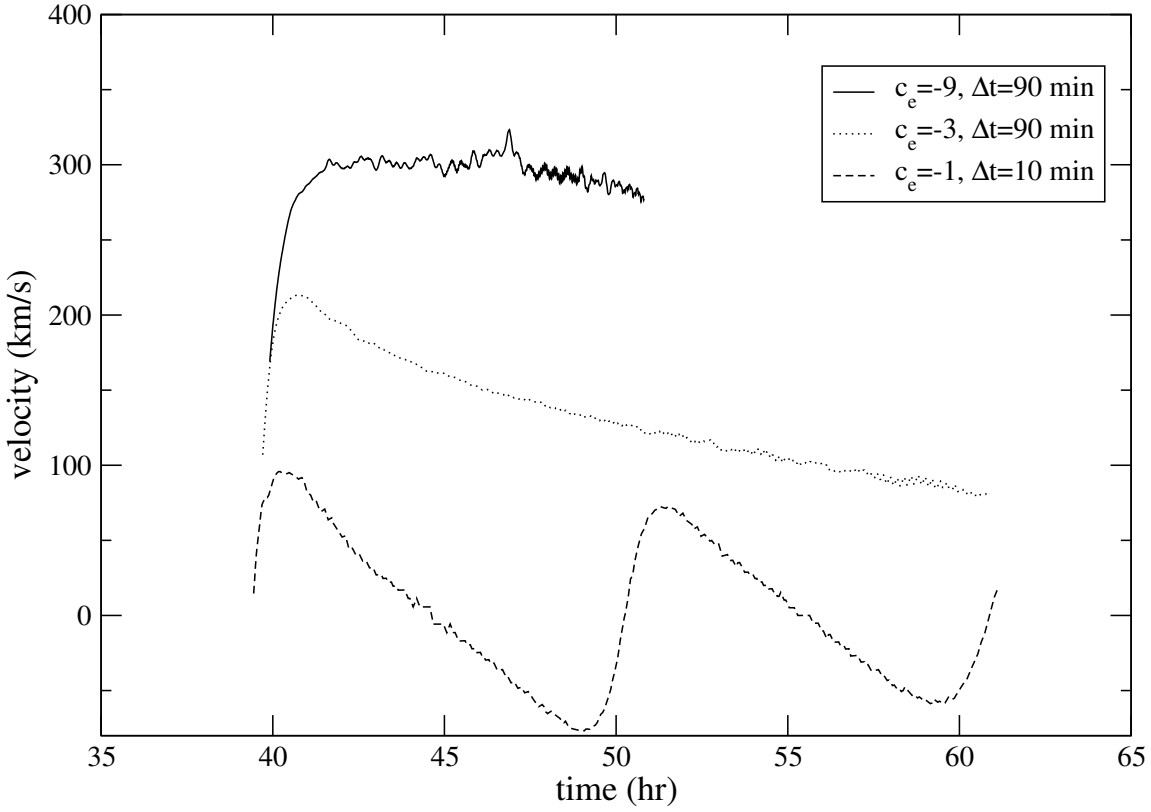

Velocity of the flux rope center vs. time

CME evolution : recent developments

- Aran et al. (2004, 2005) developed and applied a tool for rapid **predictions of proton flux and fluence profiles** observed during gradual solar energetic particle (SEP) events, for the upstream part of the shock (SOLPENCO)

$\Rightarrow$ contains data base with set of IP scenarios for SEPs, defined by the
(1) *heliolongitude* of the parent solar activity (from E75 to W90)
(2) *position of the observer* (either at 0.4 AU or 1.0 AU) and
(3) *initial shock velocity* (between 750 km/s and 1800 km/s at 18 solar radii) of the simulated shock

Recent developments (cont.)

- Fry et al. ('03,'04,'05) used *1st generation, real-time, combined "quiet" and "event-driven" solar wind model* to examine more than 600 solar flares since 1997 (rise, maximum, and decline of Solar Cycle 23) that were accompanied by metric radio Type II radio bursts and/or by partial or full halo CMEs...

⇒ experience in forecasting the flare-shocks' times of arrival (and, by implication, the following ICMEs), was summarized by discussing several specific cases, including the April/May 2001 and Halloween 2003 extreme events (Sun et al. ('03), Dryer et al. ('04), Wu et al. ('05a))

Recent developments (cont.)

- Wu et al. ('05b) also developed a data driven 3D MHD model to investigate the non-potentiality of active-region corona (innovative t-dependent projected characteristic BCs)
- Wu et al. ('04) examined the Low and Zhang (2002) suggestion that the two types of CMEs (i.e. constant speed (fast) and accelerated (slow)) are caused by the initial magnetic topology

$\Rightarrow$ simulation shows that, in addition to the magnetic topology, the *solar surface condition also plays an important role to determine the two types of CMEs*

CME evolution up to 30 $R_\odot$: creating shocks

Simple CME model

- evolution normal/inverse CMEs (Low & Zhang (2003)) confirmed
- effect SW quantified
- initial magnetic polarity affects evolution path

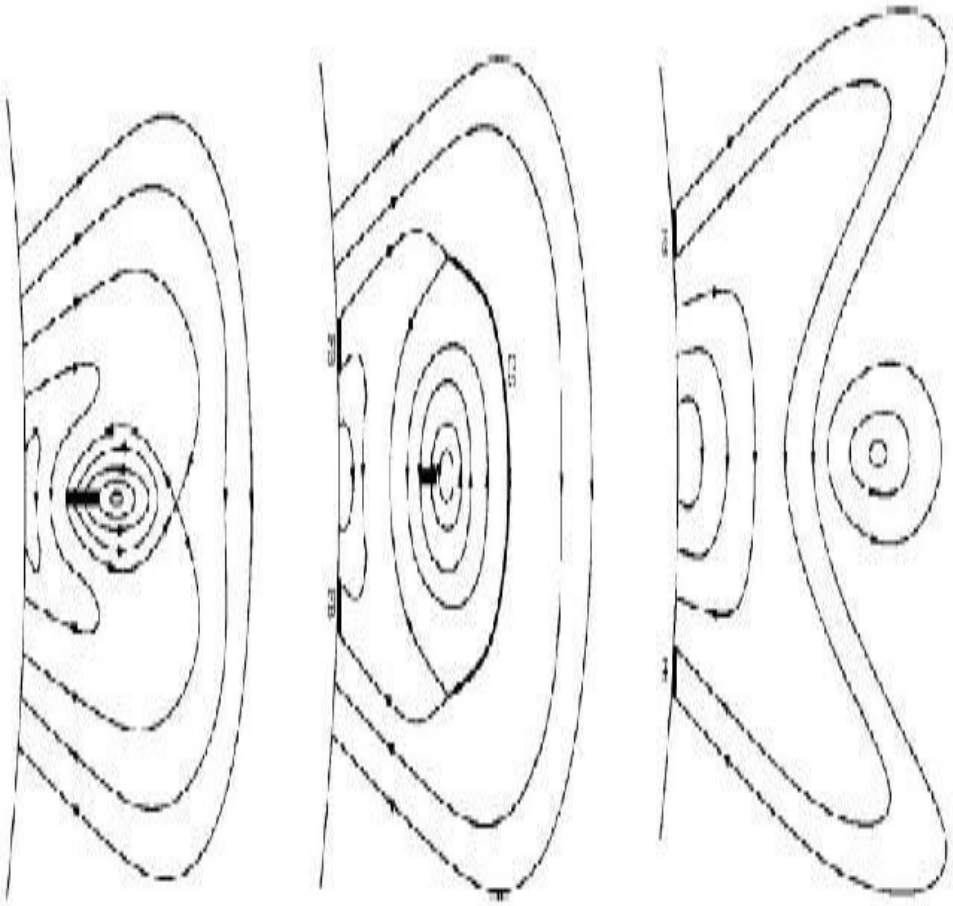

Evolution of a 'normal' CME

CME evolution up to 30 $R_\odot$: creating shocks

Simple CME model

- evolution normal/inverse CMEs (Low & Zhang (2003)) confirmed
- effect SW quantified
- initial magnetic polarity affects evolution path

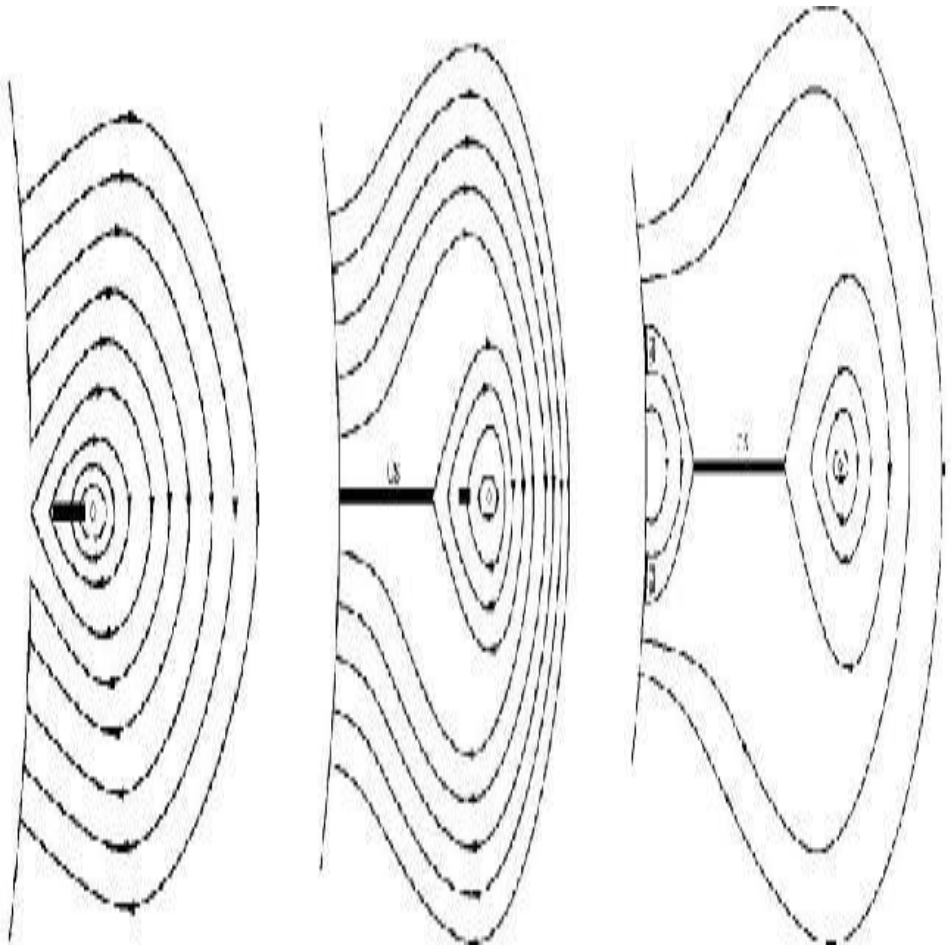

Evolution of an 'inverse' CME

CME evolution up to 1 AU

- self-similar evolution stops beyond 30 $R_\odot$
- difference normal/inverse polarity much smaller
  (e.g. density distr.)
- higher wind density at equator leads to serious deformation (compression) of the CMEs
- only difference :
  - about 6 hrs $\neq$ in arrival time
  - orientation of field

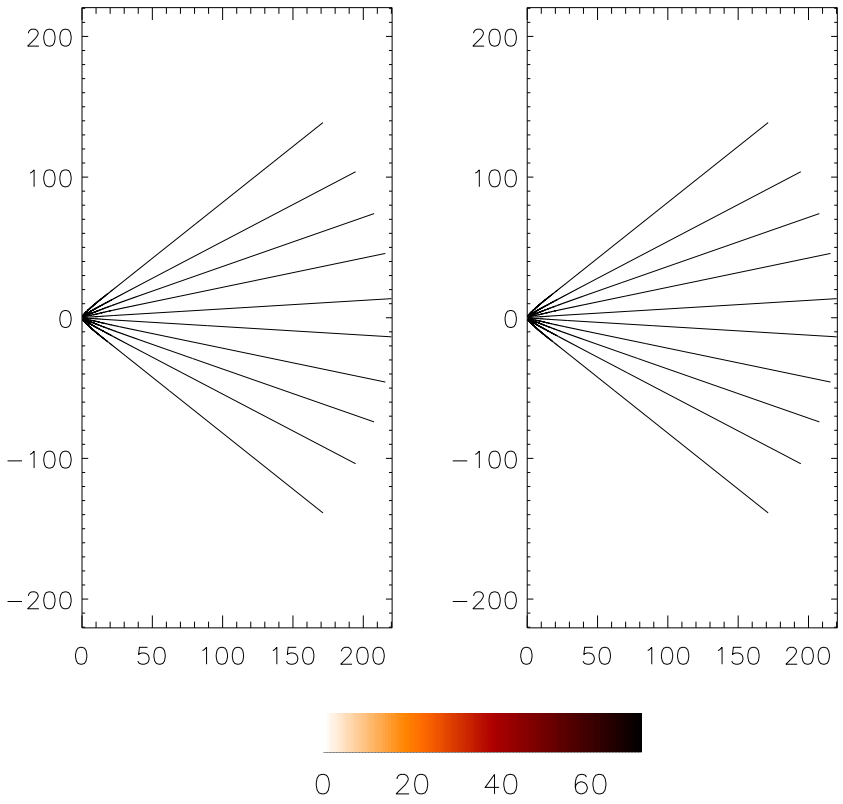

Relative density and magnetic field lines (INVERSE - NORMAL)

Simulated satellite data at 1 AU (Wind model 2)

- Normal (blue) and inverse (red) CME
- 3-part structure of CME
  1. leading shock
  2. dark cavity
  3. high density core in cavity
- leading shock front
- ...

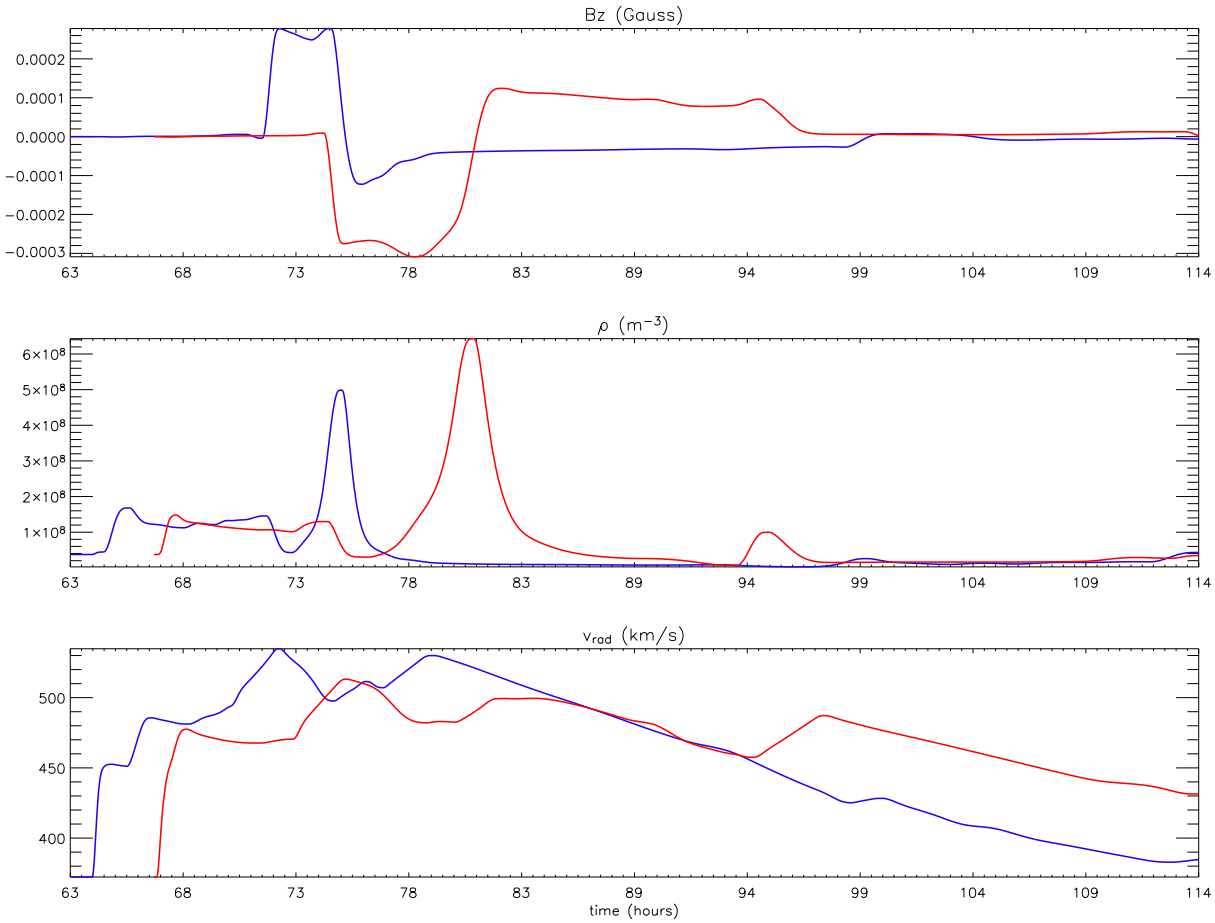

Event study

- full halo CME observed by LASCO and EIT on April 4, 2000
- observed at 16:32 UT in C2 frame
- related flare observed by EIT at 15:24 UT
- C3 measurements : plane-of-the-sky speed is 984 km/s

- try to match ACE data by
  - using wind model 2
  - playing with CME parameters (v_{cme}, θ_{cme}, B_{rope}, polarity)

Event study

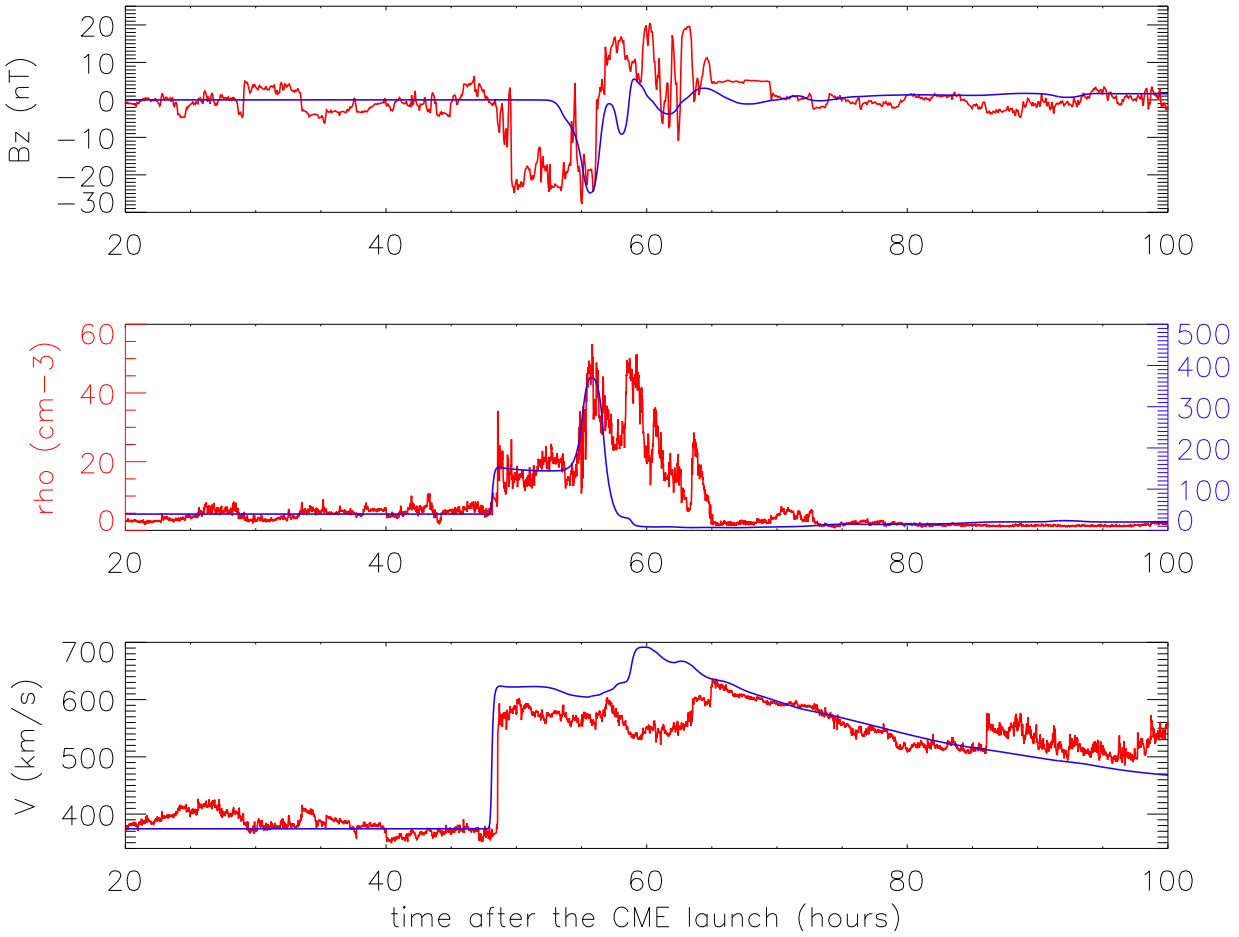

Best match : inverse CME with $v_{\mathrm{cme}} =$ 1700 km/s

However...

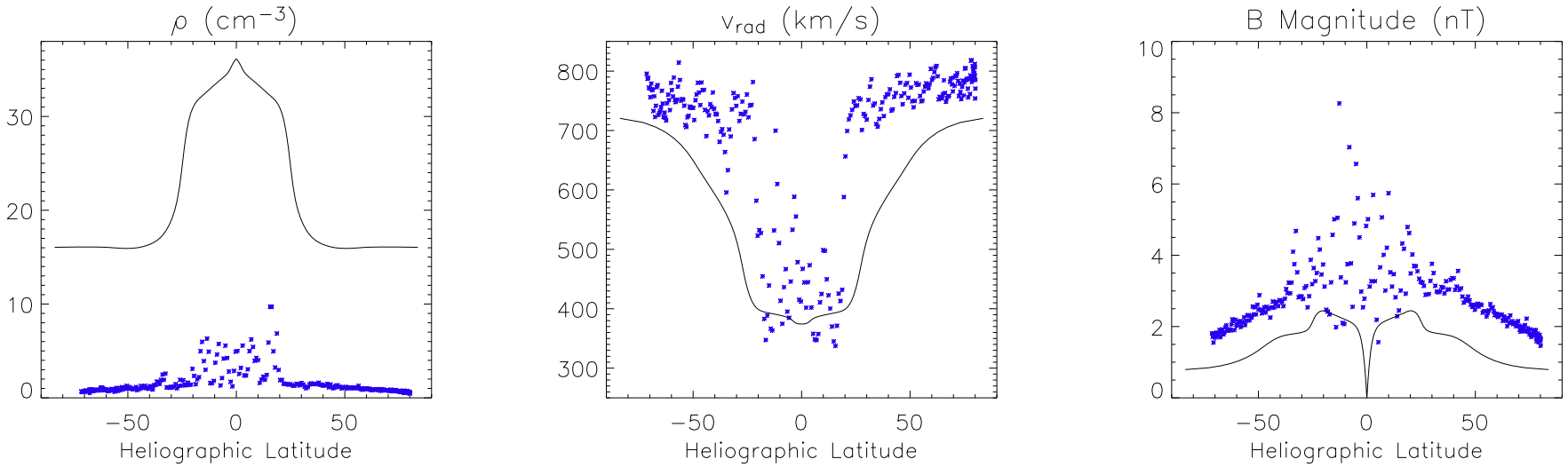

Comparison of Ulysses data (between 1/11/94 and 1/08/95, i.e. when spacecraft was evolving between 1.34 and 2.03 AU) and wind model 2 at 1 AU

Conclusions

The chosen **background wind model influences** :

- the initiation of the CME (threshold, energetics,. . .)
  - time of formation (threshold), energetics, speed, acceleration,. . .
- evolution of the CME
  - shape of leading shock front, shock speed, spread angle, mass distribution,. . .

Clearly, the initial parameters (shear velocity, polarity of fluxrope, v_{CME}, ρ_{CME}, θ_{CME},. . .) also influence the structure and evolution of the CME.

We quantified these effects and are using this knowledge for **"CME SHOCK WAVE seismology"**